Earthquake Engineering, Tenth World Conference © 1992 Balkema, Rotterdam. ISBN 90 5410 060 5

Deformation properties and shear resistance mechanism of reinforced concrete column with high and fluctuating axial force

Bernardo A. Lejano, Nobuaki Shirai, Hiromi Adachi & Arata Ono
Nihon University, Japan
Sigeyuki Amitu
Aoki Corporation, Japan

ABSTRACT: Experimental tests were conducted to evaluate the deformation properties and shear resistance mechanism of reinforced concrete column with high and fluctuating axial force. This provides some clarification on the elasto-plastic characteristics of the column. The deformation properties were studied by separating the total deformation into flexural and shear deformation components by means of flexure theory and shear theory. Furthermore, the internal concrete stress distributions were evaluated to investigate the shear resistance mechanism of reinforced concrete column. The tests reveal that the axial force greatly affects the ductility of the column.

1 INTRODUCTION

Construction of high rise reinforced concrete (RC) buildings have become prevalent even in earthquake prone areas. In the design of such structure, a special attention should be given to the lower floors' exterior columns because these columns will be subjected to high and fluctuating axial loads during strong earthquake. To evaluate the aseismic performance of RC columns under high and fluctuating axial forces, horizontal cyclic loading tests on RC columns under different axial loading conditions were conducted. The objectives of the tests are to understand the deformation characteristics and to clarify the shear resistance mechanism of RC columns.

A 30 storey residential RC building reported by Oyamatsu et al. (1990) was used as the model structure in this study. The building was designed in 3 phases, that is, the static working stress design, the ultimate strength analysis, and the static elasto-plastic analysis, in that order. The seismic design was carried out conforming to the regulations of the Architectural Institute of Japan (AIJ) and Japan's Ministry of Construction. The elasto-plastic seismic analysis conducted by Kaneko et al. (1990) showed that the axial forces of the exterior columns at the second floor were high and had the greatest fluctuation.

2 TEST METHODOLOGY

Three RC column specimens with the same dimensions and details, as shown in Figure 1, were prepared. The test specimens were 1/3.25 scale model of the second floor exterior columns. The depth (D) is 278 mm, width (B) is 278 mm, clear length (2a) is 646 mm, shear-span ratio (a/D) is 1.16, longitudinal steel ratio (ρg) is 3.94%, and the shear reinforcement ratio (ρw) is 0.89%. The yield strength (fy) is 441 MPa for the main bars and 414 Mpa for the shear reinforcing bars (hoops). The concrete compressive strength (Fc) is 46.3 MPa. The modular ratio (n) is roughly equal to 7. The specimens were named by the type of axial load applied, that is, CB060C for the constant high compressive axial load, CB070T for the constant tensile axial load, and CB07T06C for the fluctuating axial load. The specimens were subjected to cyclic horizontal forces by applying

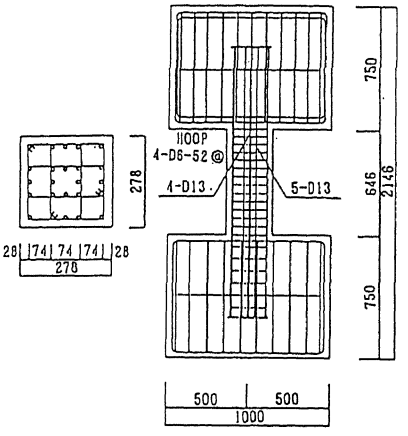

Figure 1. Detail of test specimen

Table 1. Applied axial loads

Specimen Name	Axial force ratio (η =N/BDFc)	Axial force (N) KN
CB060C	0.74	2632 *
CB070T	-0.26	-941 **
CB07T06C	-0.26 to 0.74	-941 to 2632 ***

* Nc=0.6Nuo=0.6(0.85BDFc+Asfy)
** Nt=0.7Nut=0.7Asfy
*** Nc=0.6Nuo, Nt=0.7Nut
N=0.25[BD+(n-1)As]Fc at Q=0
As=the total main reinforcing steel area of the section

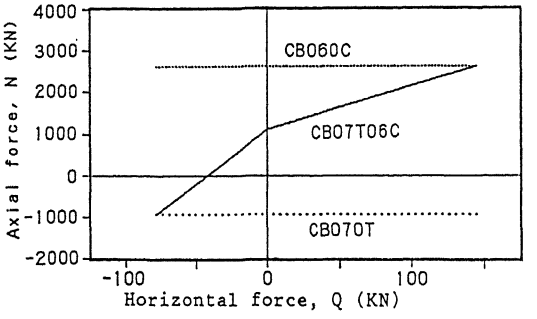

Figure 2. Q-N relationships

prescribed specimen rotation (R). The applied axial loads are listed in Table 1. Figure 2 shows the relationship between the applied axial load and horizontal load. The fluctuation of the axial force for CB07T06C was assumed based on the result of static elasto-plastic frame analysis.

Shown in Figure 3 is the loading apparatus. The axial load was applied on the upper end of the specimen using a 4900 KN hydraulic jack. Horizontal force was applied using a 1960 KN hydraulic jack anchored on a reaction wall. The horizontal force was applied through an L-type steel jig to insure that

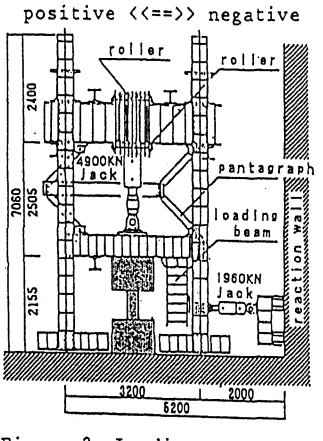

Figure 3. Loading apparatus

the inflection point is kept at the mid-height of the specimen.

The horizontal load (Q), the axial load (N), the relative horizontal displacement (δ), and the strains in the main and shear reinforcing bars were measured. The loads were measured using the load cells. Figure 4 shows the deformation measurement technique used. The horizontal deflection (δ) and total vertical displacement ($\Delta \delta v$) were measured using the displacement transducers. The clip gauges were mounted at 10 intervals on each of the two vertical broken lines to measure the axial deformation. Also, the column was divided into 4 segments. The longitudinal, lateral, and diagonal deformations of each segment were measured using the clip gages. The strains of the main and shear reinforcing bars were measured using the strain gauges with the gauge length of 2 mm.

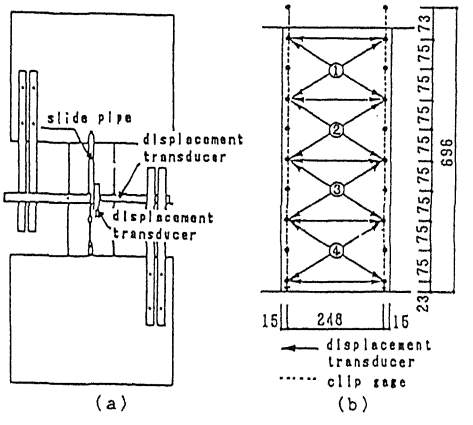

Figure 4. Deformation measurement system

To obtain a detailed and reliable measurement of deformations, the horizontal load was monotonically applied to the specimen up to a member rotation of R=9/1000 (δ =5.81 mm) at which maximum strength was expected to be attained. One cycle of loading is accomplished by forcing the specimen up to the prescribed rotation (positive loading) and afterwards reversing it into the opposite direction with the same amount of rotation (negative loading). The cyclic loading was repeated five times at this member rotation. After that, the rotation was gradually increased until the final failure was reached.

3 TEST RESULTS

Figure 5 shows the horizontal force - horizontal displacement (Q- δ) relationship of each specimen along with the corresponding final crack patterns. As observed, the crack propagation and horizontal load carrying capacity are greatly affected by the axial

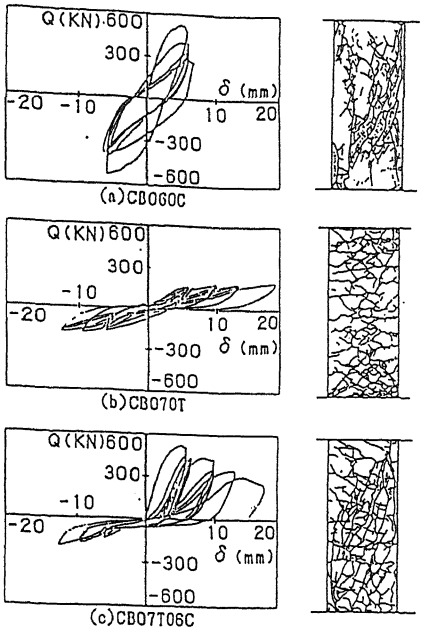

Figure 5. Q- δ relationship and crack pattern

load. The tensile axial load tends to produce lateral cracks and causes larger horizontal deflection as exhibited by CB070T. On the other hand, the compressive axial load tends to cause brittle failure as observed in CB060C. However, brittleness is noticeably reduced by the fluctuation of axial load as in CB07T06C.

Figure 6 shows the relationship between the horizontal force (Q) and axial deformation (Δ δ v) of each specimen. The amount and variations of Δ δ v differ for each specimen. For the specimens with constant axial force (CB060C and CB070T), Δ δ v does not vary much as Q increases, but increases significantly as the number of cycle increases. On the contrary, for the specimen with fluctuating axial force (CB07T06C), Δ δ v does not change much as the number of cycle increases, but significantly varies at the reversal in the direction of axial load (from compression to tension, and vice-versa).

Figure 7 shows the horizontal force - lateral strain (Q- εh) relationships of each specimen. The lateral strain was evaluated

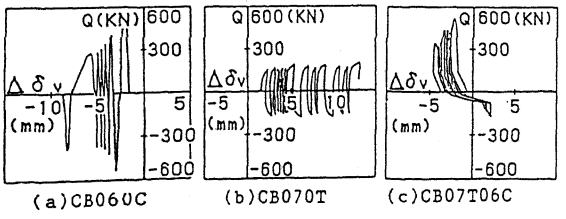

Figure 6. Q-Δ δ v relationships

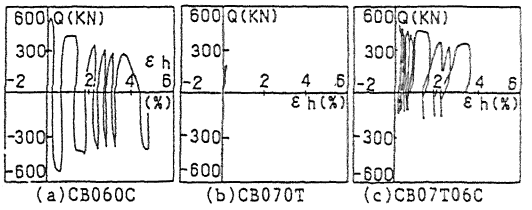

Figure 7. Q- εh relationships

from the measured lateral deformation of segment 2. εh of CB070T is very small. On the other hand, εh of CB060C and CB07T06C, especially the former, is significantly large.

The tensile yielding of the hoops were observed near the peak loads at the negative loading of CB060C and at the positive loading of CB07T06C. Therefore, it is presumed that the confining effect of the hoops was lost near the peak load and consequently caused a remarkable deterioration of concrete.

4 EVALUATION OF DEFORMATION PROPERTIES

The deformation properties of RC columns were evaluated using two methods, namely, the flexure theory and the shear theory.

4.1 Flexure theory

The flexural deformation component (δ f) can be calculated by integrating the curvature distribution along the member length. The curvature distribution was obtained by evaluating the average curvature of each of the 10 intervals along the member axis based on the measured axial deformations along the two vertical broken lines depicted in Figure 4(b). Then, the shear deformation (δ s) is defined as the difference between the total and flexural deformation (δ s= δ - δ f).

4.2 Shear theory

The strain states in each segment (Figure 4(b)) can be evaluated from the measured lateral, longitudinal, and diagonal deformations. However, the strains caused by the bending moments are still coupled with those caused by the axial and shear forces. The following is a method of uncoupling the flexural strains. The schematic deformation condition of a segment is shown in Figure 8. Normally, condition (a) is produced in columns. The flexural component is obtained by subtracting the deformation of condition (b) from the deformations of condition (c). Then, the flexure component is subtracted from the deformations of condition (a) to arrive at condition (d). If the axial deformation, Δ Ty, along the neutral axis is known, the

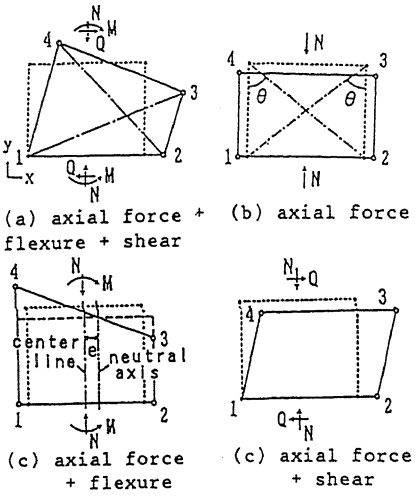

Figure 8. Schematic configuration of deformation of column segment

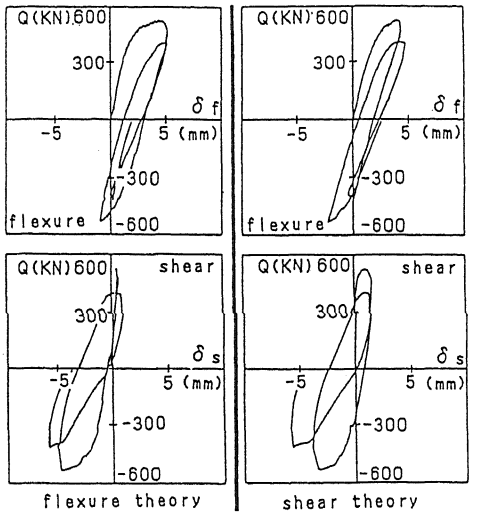

Figure 9. Q-δ f and Q-δ s relationships

corresponding lateral deformation, Δ Tx, and diagonal deformations, Δ T13 and Δ T24, as well as the strain ε x, ε y, ε 13, and ε 24 can be obtained from the measured deformations Δ 112, Δ 143, Δ 123, Δ 113, and Δ 124 as follows:

$$\varepsilon y = \Delta Ty/114 : \quad \varepsilon x = \Delta Tx/112 = (\Delta 112 + \Delta 143)/(2\ 112)$$

$$\varepsilon 13 = \Delta T13/113 = \{\Delta 113 - (\Delta 123 - \Delta Ty)\ \mathrm{Cos}\,\theta\}/113$$

$$\varepsilon 24 = \Delta T24/124 = \{\Delta 124 - (\Delta 114 - \Delta Ty)\ \mathrm{Cos}\,\theta\}/124$$

Δ Ty was evaluated by the fiber method (Kanda et al.(1988)) with the measured axial forces and curvatures as the input parameters. The Mohr's strain circle was drawn based on these strains. Then the strain state (ε x, ε y, γ xy) of condition (d) was evaluated. The shear deformation component, δ s, was obtained by summing up the product of γ xy and the corresponding length of each segment. Furthermore, the flexural deformation component was obtained by subtracting δ s from the total deformation.

4.3 Results of deformation evaluation

Figure 9 shows the horizontal force - flexural deformation (Q-δ f) curves and the horizontal force - shear deformation (Q-δ s) curves for CB060C. Relatively, similar hysteresis curves were obtained from the flexure theory and shear theory. The flexural deformation components tend to accumulate during the positive loading. Conversely, the shear components tend to accumulate during the negative loading. This may be due to the deterioration of the flexural stiffness during the positive loading and consequently leaves residual flexural deformation. Also, the axial compressive strain at both ends of the column reached 0.00343 at the peak load, exceeding the strain at the compressive strength of concrete (ε o=0.00267). While at the negative loading, the shear stiffness greatly deteriorated. This may be caused by the diagonal cracks formed during the negative loading crossing the cracks previously formed during the positive loading.

Next, the ratios of flexural to total deformation (δ f/ δ) for CB060C and CB07T06C were compared. Figure 10 shows the variations of δ f/ δ as the horizontal displacement is increased. The results obtained through the flexure theory and shear theory are almost identical. The flexural component is observed to be dominant. The ratios, δ f/ δ , for the specimens C-2 and C-3 reported by Ushimaru et al. (1990) are also plotted in the figure for comparison. The construction details of C-2 and C-3 are identical with the specimens

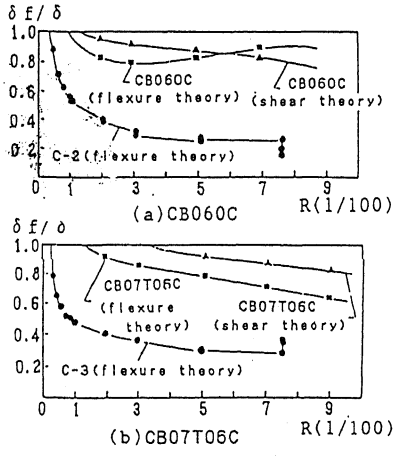

Figure 10. R - δ f/ δ relationship

presented in this report. However, the horizontal loading method adopted was different, that is, C-2 and C-3 were tested under gradually increasing cyclic loads before reaching the peak load. The ratios, $\delta f/\delta$, for C-2 and C-3 are very low compared with the current specimens. This may be attributed to the observed deterioration at an early stage of the shear stiffness of C-2 and C-3.

Figure 11 shows the distribution of flexural (δf), shear (δs), and axial ($\Delta \delta v$) deformations of CB060C along the member axis at R=±9/1000 at the first load cycle. As expected, the flexural deformations are small near the mid height and are largely concentrated near the top and bottom of the column. The same behavior was observed in the other specimens. The shear deformations are almost uniformly distributed along the member axis at the positive loading. However, the shear deformations tend to enlarge at the mid height of the column at the negative loading. On the other hand, CB070T and CB07T06C had bigger shear deformations near the base of the column than near the mid height at R=+9/1000. Although the axial deformation distribution is not uniform, no significant pattern can be observed.

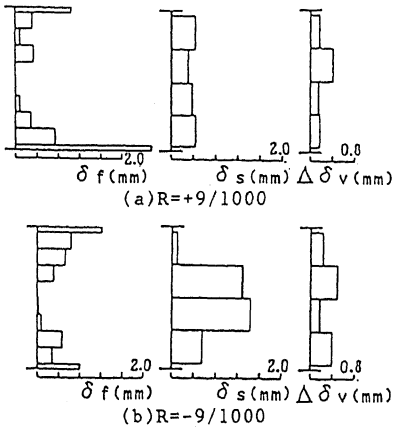

Figure 11. Distribution of δf, δs, and $\Delta \delta v$ along the member axis of CB060C.

5 EVALUATION OF SHEAR RESISTANCE MECHANISM

To clarify the shear resistance mechanism of RC columns, the internal concrete stress distribution of the specimen have been evaluated based on the flowchart shown in Figure 12. The evaluation is divided into two processes. In the first process, each segment (see Figure 4(b)) was subdivided into eight slices along the depth. Flexural analysis was performed by means of the fiber method to obtain the axial stress of each slice (σy). In the second process, the shear theory was used to evaluate the lateral stress (σx) and

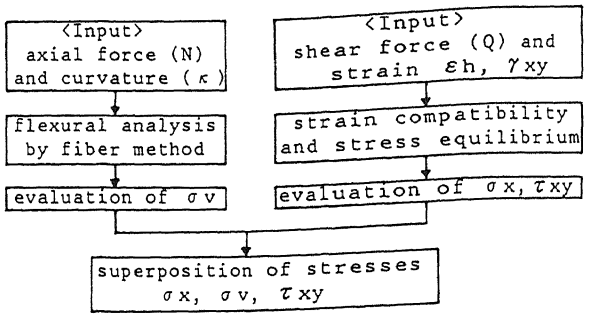

Figure 12. Stress evaluation technique

shear stress (τxy). Finally, the stress distribution of the specimen was obtained by superimposing, slice by slice, the stresses obtained from the two processes.

Figure 13 shows the principal compressive stress distributions with the corresponding crack patterns of CB060C and CB07T06C at the peak positive load. It can be seen that an arch action is formed, and the width of the strut of the arch is relatively wide. Also, the inclination of the cracks corresponds to the direction of the principal compressive stress.

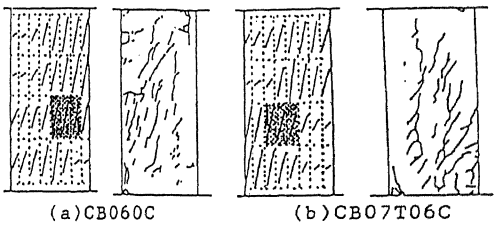

Figure 13. Distribution of principal compressive stresses at the peak positive load

Figure 14 shows the principal compressive stress - principal compressive strain (σd-εd) relationships for the shaded slices at segment 3. The variations of the angle between the principal stress directions and the member axis (α) are also plotted in the figure. The σd- εd relationships of both

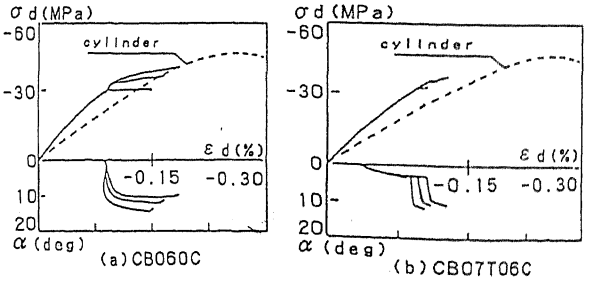

Figure 14. σd- εd relationships

specimens behave similarly to the stress-strain curve of concrete cylinder. However, the σd- εd relationships have a somewhat higher stiffness and the maximum compressive stresses did not reach the compressive strength of concrete. The effectiveness factor for the compressive strut, υ, that is, the ratio of the maximum principal compressive stress to the compressive strength of concrete, was evaluated to be υ=0.75 for CB060C and υ=0.74 for CB07T06C. The angle α was evaluated to be α=12.2° for CB060C and α=11.5° for CB07T06C when the maximum principal compressive stresses were attained.

In Figure 15, υ is plotted against the ratio of principal strains, $|\varepsilon dt/\varepsilon d|$, where εdt is the principal tensile strain and εd is the principal compressive strain. The test results and formula for υ by Collin's et al. (1982) are also plotted in the figure. The values of υ of the present study agree well with Collin's test results and formula.

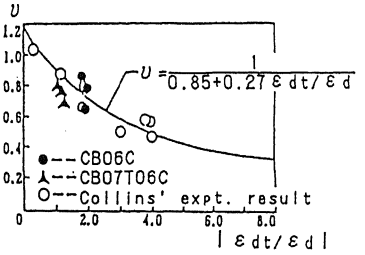

Figure 15. υ - $|\varepsilon dt/\varepsilon d|$ relationship

Lastly, the AIJ guideline formula (Architectural Institute of Japan (1988)) for the ultimate shear strength (Vu) of RC columns is applied to CB060C. The AIJ formula was derived on the basis of the lower bound theory of plasticity under the hypothesis that the shear resistance mechanism is composed of the arch and truss action. The AIJ's method A predicts υ=0.46, α=11.9° and Vu=479 KN while the AIJ's method B predicts υ=0.83, α=11.9°, and Vu=481 KN. The value of Vu from the test results were 517 KN at the positive loading and 543 KN at the negative loading. Methods A and B underestimate Vu since both methods do not consider the effect of high axial force.

CONCLUSION

Based on the tests and evaluations conducted, the following conclusions may be said.

As the axial load becomes excessive, the axial and lateral deformations become large and cause the deterioration of concrete. Consequently, this reduces the ductility of RC columns.

It is possible to separate the total deformations into flexural and shear deformation components based on the flexure and shear theories. It was found that the ratios of the deformation components to the total deformation and the deterioration of flexural stiffness and shear stiffness depend on the loading history.

The axial stresses due to the axial forces and the bending moments can be evaluated by the fiber method. The shear stresses and the lateral stresses caused by the shear forces can be evaluated by the shear theory. The internal stress distribution of concrete in RC columns can be simulated by superimposing the stresses stated above. The internal stress distribution offers explanation about the shear resistance mechanism of RC columns such as the arc action observed.

REFERENCES

Amitu, S., et al. 1990. Part 7: Studies on elasto-plastic behavior of reinforced concrete column with fluctuating axial force. Annual Report of the Architectural Institute of Japan: 863-864.(in Japanese)

Architectural Institute of Japan 1988. Design guideline for earthquake resistant reinforced concrete buildings based on ultimate strength concept: 104-150. (in Japanese)

Kanda, M., et al.1988. Analytical study on elasto-plastic hysteretic behavior of reinforced concrete members. Transaction of the Japan Concrete Institute. Vol.10: 257-264.

Kaneko, E., et al. 1990. Part 4: Studies on elasto-plastic behavior of reinforced concrete column with fluctuating axial force. Annual Report of the Architectural Institute of Japan: 857-858. (in Japanese)

Oyamatsu, T., et al. 1990. Part 3: Studies on elasto-plastic behavior of reinforced concrete column with fluctuating axial force. Annual Report of the Architectural Institute of Japan: 855-866. (in Japanese)

Ushimaru, Y, et al. 1990. Part 5: Studies on elasto-plastic behavior of reinforced concrete column with fluctuating axial force. Annual Report of the Architectural Institute of Japan: 859-860. (in Japanese)

Vecchio, F. and M.P. Collins 1982. The response of reinforced concrete to inplane shear and normal stresses. ISBN Pub. No.82-03. University of Toronto.